Biochemistry and Biophysics Reports 4 (2015) 306–311

Contents lists available at ScienceDirect

Biochemistry and Biophysics Reports

journal homepage: www.elsevier.com/locate/bbrep

Characterisation of the flavin adenine dinucleotide binding region of *Myxococcus xanthus* protoporphyrinogen oxidase

Mavis O. Boateng [a], Anne V. Corrigall [a], Edward Sturrock [b], Peter N. Meissner [a,b,*]

[a] Lennox Eales Porphyria Laboratories, Department of Medicine, University of Cape Town Medical School, K-floor, Old GSH Main Building, Observatory, Cape Town 7925, South Africa

[b] Division of Medical Biochemistry, Department of Integrative Biomedical Sciences, Institute of Infectious Disease and Molecular Medicine, and Structural Biology Research Unit, University of Cape Town, Observatory, Cape Town 7925, South Africa

ARTICLE INFO

Article history:
Received 28 July 2015
Received in revised form
12 October 2015
Accepted 13 October 2015
Available online 29 October 2015

Keywords:
Porphyria
Protoporphyrinogen oxidase
FAD
Myxococcus xanthus
Haem synthesis

ABSTRACT

Protoporphyrinogen oxidase (PPOX), the penultimate enzyme in the haem biosynthetic pathway catalysers the six electron oxidation of protoporphyrinogen-IX to protoporphyrin-IX, in the presence of flavin adenine dinucleotide (FAD) and oxygen. In humans, partial defects in PPOX result in variegate porphyria. In this study, the FAD binding region in *Myxococcus xanthus* PPOX was analysed by engineering and characterising a selection of mutant proteins. Amino acid residues which interact with FAD via their side chains were selected for study. Mutants were characterised and compared with wild type protein. Characterisation included FAD quantitation, analysis of FAD spectra and kinetic assay. Results revealed that Serine 20 mutants could still bind FAD, but polarity in this position is favourable, yet not essential for the integrity of FAD binding. Study of Glutamate 39 mutants suggest that a negative charge at position 39 is clearly favoured for interaction with the ribose ring of FAD, as all non-conservative replacements could not bind sufficient FAD. Asparagine 441 appears not to be directly involved in FAD binding but rather in stabilizing the FAD, and polarity in this position appears important. Tryptophan 408 may play a role in orientating or stabilizing the bound substrate during catalysis, and a non-polar (or slightly polar) residue is favoured at this position; however, aromaticity in this position appears not to be critical. Overall this study sheds further light on how *M. xanthus* PPOX interacts with FAD.

1. Introduction

PPOX (E.C. 1.3.3.4), the penultimate enzyme in the haem biosynthetic pathway catalyses the removal of electrons from protogen to form proto aided by a FAD cofactor [1]. To form proto, electrons are removed, starting with two electrons moving from the tetrapyrrole ring of the substrate to reduce the FAD, which in turn oxidises the final electron acceptor (O_2) forming H_2O_2 in the process. This desaturation step occurs three times resulting in the removal of a total of six electrons from protogen to form proto and three H_2O_2.

PPOX structures from four species have been resolved to date, including the human structure [2–5]. These structures provide new insight into the structure–function properties of this enzyme and suggest that all the electrons in the reaction are lost from a single point in the tetrapyrrolic macrocycle, based on the lack of space for the substrate to rotate in the active site [2,3]. The precise orientation of the substrate in the active site remains unclear as no structure including the protogen substrate has been resolved to date, although modelled substrate has been shown. However, the positioning of the FAD is clear from the resolved structures, which reveal a tri-lobed protein including a FAD-binding domain of the *p*-hydroxybenzoate hydroxylase-type fold; a substrate-binding domain enclosing a narrow active site cavity beneath the FAD; and an alpha-helical membrane-binding domain.

Defects in the gene (*PPOX*) encoding this enzyme result in reduced enzyme activity, and may lead to the characteristic accumulation of haem precursors as well as porphyrin(ogen)s associated with VP in humans [6]. To date, 170 VP-causing mutations have been reported in the Human Gene Mutation Database. In some cases reduced enzyme activity has been attributed to inferior

Abbreviations: VP, variegate porphyria; PPOX, protoporphyrinogen oxidase; HPPOX, human protoporphyrinogen oxidase; MxPPOX, *Myxococcus xanthus* protoporphyrinogen oxidase; BsPPOX, *Bacillus subtilis* protoporphyringen oxidase; NtPPOX, *Nicotinia tabacum* mitochondrial protoporphyrinogen oxidase; proto, protoporphyrin-IX; protogen, protoporphyrinogen-IX

* Corresponding author at: Lennox Eales Porphyria Laboratories, Department of Medicine, University of Cape Town Medical School, K-floor, Old GSH Main Building, Observatory, Cape Town 7925, South Africa.

E-mail address: peter.meissner@uct.ac.za (P.N. Meissner).

http://dx.doi.org/10.1016/j.bbrep.2015.10.006

protein–FAD interaction and earlier reports on some VP-associated mutations have shed light on the binding properties of FAD in PPOX [7,8]. Based on the published structures and *in silica* predictions [9], mutants have been engineered in which various residues interacting with the cofactor, FAD, were mutated, and their effect on FAD binding and/or change in orientation reported. We also considered earlier work by Maneli et al. [10] which demonstrated that certain residues are critical for FAD binding. Specifically, characterisation of HPPOX mutants, Gly9Ala and Gly11Ala, revealed that FAD was unable to bind in these mutants, whereas a Gly14Ala mutant bound FAD poorly, suggesting that PPOX, like other enzymes with characteristic FAD-binding regions, has a sensitive, co-ordinated interaction with FAD.

Thus, in this study we further characterise the FAD binding region in PPOX by engineering and characterising a selection of relevant mutants based on the *Myxococcus xanthus* form of the enzyme. As the FAD binding region is highly conserved amongst flavoproteins [11,12], it is likely to interact similarly with FAD in different species of PPOX, including MxPPOX, as well as non-related flavoprotein oxidases.

2. Materials and methods

Myxoccocus PPOX plasmid was kindly donated by Professor H. A. Dailey, University of Georgia, Athens, GA, USA. For mutagenesis, the QuickChange site-directed mutagenesis system from Stratagene was used. Direct sequencing was performed by the core DNA sequencing facility of the University of Stellenbosch, South Africa, using the ABI-3100 Auomated Genetic Analyser and a Big Dye version 3.0 kit (Applied Biosystems, Brachberg, USA). The sonicator (model XL2020) utilised was from Heat Systems, Framington, NY, USA. TALON metal affinity resin was obtained from Clonetech laboratories, Palo Alto, CA, USA. The Hybaid Omnigene thermal cycler was from Teddington, UK. Spectrophotometric measurements were performed on a Hitachi U-3200 UV/vis spectrophotometer from Koki Co. Ltd., Tokyo, Japan. Fluorimetric measurements were performed on a Hitachi 650-10S fluorescence spectrophotometer, Koki Co. Ltd., Japan.

2.1. Selection of mutants

For selection of relevant amino acid residues (i.e. those with potential to play a role in the binding of FAD), protein–FAD interaction was analysed in the MxPPOX crystal structure with and without bound acifluorfen inhibitor (PDB2IVD and PDB2IVE, respectively) using the software packages LigPlot and PyMol. Published PPOX structures generally include the well-known herbicidal competitive inhibitor acifluorfen in the active site, as natural substrate (protogen) is unstable. Structures with acifluorfen therefore assist our understanding of active site interactions. Conservation of selected residues was assessed by multiple sequence alignment using BioEdit. MxPPOX residues Ser-20, Glu-39, Trp-408 and Asn-441 were mutated.

2.2. Site-directed mutagenesis

Mutants were engineered according to manufacturer's instructions. A selection of single colonies was screened by restriction analysis, where possible. The oligonucleotide primers used in the mutagenesis, and restriction enzymes, are available on request. Restriction enzyme digests were analysed on a 6% non-denaturing polyacrylamide gel to identify positive clones. In positive clones the entire MxPPOX cDNA was sequenced to ensure the correct insertion of the mutation, as well as the absence of any erroneous mutations (primers available on request).

2.3. Expression and purification of wild type and mutant MxPPOX

Wild type MxPPOX with a 6 × His tag in a tac promoter-driven expression plasmid was transformed in our laboratories into competent *JM109* cells. One ml of 30 % glycerol stock of MxPPOX was inoculated in 1 L Luria broth (LB), containing 100 μg/ml ampicillin and incubated for 22 h at 30 °C with shaking (225 rpm). Mutant MxPPOX *JM109* cells were expressed under the same conditions as wild type.

Cells from the overnight culture were harvested by centrifugation (3000*g*) for 30 min at 4 °C. The pellet was resuspended in 30 ml sonication buffer (0.02 M Tris/HCl, 0.1 M NaCl, 1% Tween 20, pH 8.0). Cells were then lysed/sonicated at 60 W for 30 s × 4 with intermittent cooling on ice. The lysate was centrifuged at 105,000*g* for 40 min at 4 °C. The supernatant was loaded onto a column (0.9 × 30 cm) containing 600 μl TALON resin, pre-equilibrated in 10 ml sonication buffer. The flow through was collected at a flow rate of 15 ml/h. The column was washed with at least 10 ml of wash buffer (0.02 M NaH_2PO_4, 0.1 M NaCl, 0.5 % Tween 20, 10% glycerol, 0.025 M imidazole, pH 6.3) prior to eluting with elution buffer (0.05 M NaH_2PO_4, 0.1 M NaCl, 0.5 % Tween 20, 10% Glycerol, 0.15 M imidazole, pH 7.0). A final concentration of 1 μg/ml PMSF was added throughout the purification procedure. Purification of the proteins was assessed on 7.5–17.5% gradient SDS-PAGE. Protein was quantitated using the Bio-Rad protein microassay with BSA as protein standard.

2.4. PPOX assay

PPOX activity was assessed by measuring product (proto) formation spectrofluorimetrically as previously described [10]. Assays were performed at 37 °C and at pH 8.1.

Kinetic constants K_M and k_{cat} were extrapolated from substrate–velocity plots using an iterative Gauss Newton curve fitting procedure.

2.5. Determination of $T_{½}$

$T_{½}$s were determined by incubating aliquots of enzyme at a specific temperature ranging from 30 to 65 °C for 5 min then placing on ice immediately. Specific activity was then determined (at excess substrate concentration). $T_{½}$ was calculated graphically by plotting temperature versus velocity.

2.6. The effect of pH on activity

The effect of pH on activity was determined over the pH range 6–9 using phosphate (pH range 6–7) and Tris/HCl (pH range 7–9) buffers.

2.7. Spectral analysis

FAD was quantitated by measuring absorption at a wavelength of 450 nm in a UV/vis absorption spectrophotometer. Absorbance at 450 nm was expressed as $OD_{450\ nm}$/mg protein/ml as previously reported [10,13]. To analyse the potential effects of the mutations on FAD binding, PPOX UV/vis spectra were recorded from 550 nm to 250 nm.

3. Results and discussion

3.1. PPOX protein sequence and structural analysis

Alignment of MxPPOX with 19 prokaryote, HPPOX and NtPPOX protein sequences, confirmed the consensus sequence of the FAD

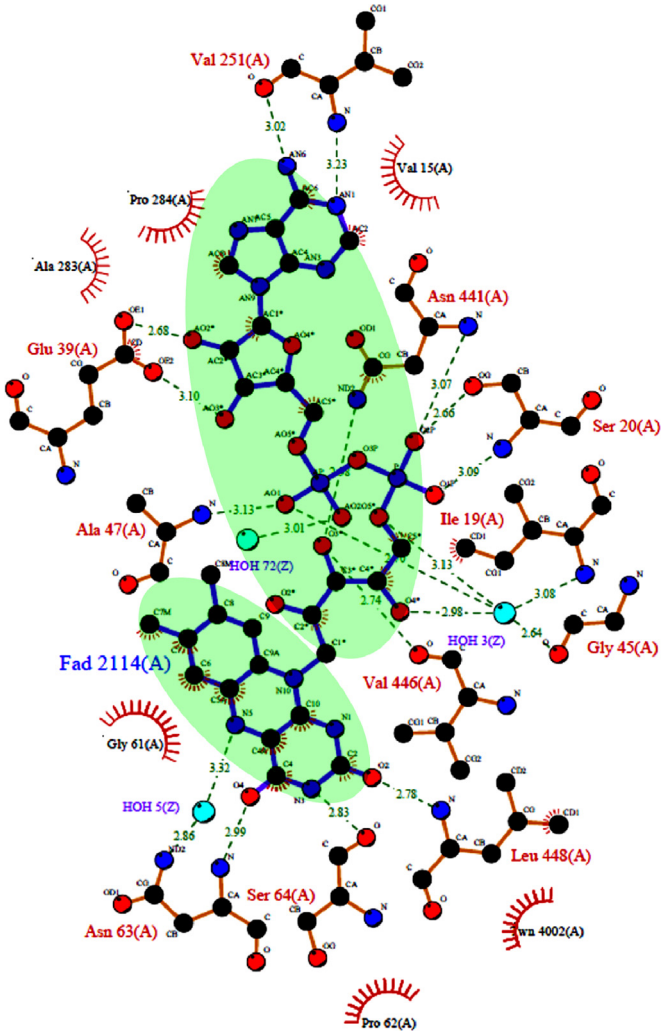

Fig. 1. LigPLot representation of the FAD (highlighted in green) binding site in subunit A of mxPPOX (PDB: 2IVE) [3]. Black=carbon; blue=nitrogen; red=oxygen; purple=phosphate; cyan=water molecule. Polar interactions are shown as dotted lines and hydrophobic interactions are shown as "eye lashes".

superfamily reported previously by Dailey and Dailey [11] (data not shown). Residues Ser-20 and Glu-39 of MxPPOX are part of this consensus sequence and are highly conserved. This suggests the importance of their interaction with FAD. Furthermore, Asn-441 is another highly conserved residue among the prokaryotic PPOXs.

A tryptophan residue is normally seen in protein structures of the FAD superfamily interacting with the hydrophobic ring of the FAD isoalloxazine ring [14,15]. In mxPPOX, the positioning of Trp-408 is further away from the isoalloxazine ring, suggesting that in mxPPOX, Trp-408 could have an alternative role (Fig. 1). Nevertheless, examination of the alignment suggests that an aromatic ring is favoured in this position.

Protein–ligand interaction in MxPPOX structure revealed that the three conserved residues (Ser-20, Glu-39 and Asn-441) interact with FAD via their side chains (Fig. 1), hence, they could possibly be playing a role in the binding and orientation of FAD. The Ser-20 side chain makes three interactions with the phosphate group (phosphate group 1) of FAD (the third interaction is only visible in 3-D view). The Glu-39 side chain has two carbonyl groups that interact with the hydroxyl group of the ribose ring. Asn-441 is located in a long loop that twists perfectly to orientate the Asn-441 residue to interact with the phosphate group 2 of FAD via its side chain and the amino group with the ribityl chain of the

Table 1
Purification yield and activity of wild type and mutant MxPPOXs.

PPOX	Yield of PPOX from 1 L of culture (mg)	Specific activity (μmol/mg/min)	Percentage of wild type activity
Wild type	3.45	71.3	100
Ser20Ala	0.47	5.0	7
Ser20Thr	2.67	7.1	10
Glu39Asp	2.02	13.6	19
Glu39Ala	0.33	0	0
Glu39Lys	4.68	0.1	0
Glu39Gln	0.63	0	0
Trp408Leu	1.34	37.2	52
Trp408Tyr	5.80	12.5	18
Asn441Gln	1.90	19.3	27
Asn441Ile	0.30	11.5	16

FAD. Due to the fact that side chain interactions allow for more movement compared to backbone interactions, it is tempting to speculate that flexibility at both the ribose and phosphate regions of FAD could be important, benefitting protein–FAD association.

3.2. Expression and mutagenesis

In this study pure, soluble forms of wild-type and relevant mutant MxPPOXs were required for analysis and characterisation. A series of ten mutant MxPPOXs were successfully engineered, expressed, and purified using metal affinity chromatography at 4 °C. The mutants were chosen based on relevant replacements of the 4 residues of interest (Ser-20, Glu-39, Asp-441 and Trp-408) (Table 1). Four mutants had very low expression yields compared to wild type. IPTG induction had no effect on expression (data not shown). However, growth at 30 C (rather than at 37 °C) improved expression and yield was increased by doubling the number of cells inoculated in 1 L growth media. Growth time was minimised (18 h) to prevent the production of insoluble inclusion bodies [16]. Specific activities of the mutants ranged from 0 to 52% of wild-type activity. Those with zero, or very low activity (Glu39Ala/Lys/Gln) could not be kinetically characterised further.

3.3. Cofactor and kinetic characterisation

FAD–PPOX interaction was assessed by analysing the binding properties of FAD in both mutants and wild type MxPPOX (Fig. 2). Furthermore, the activity and kinetic parameters of the mutant PPOXs were analysed and compared to wild type (Table 2).

FAD in solution displays typical UV/vis spectra with peaks at 450 nm and 375 nm. Wild type MxPPOX has this typical FAD spectrum (data not shown). The 450 nm peak is higher than the 375 nm peak indicating an oxidised FAD, and is in keeping with earlier FAD PPOX studies [10,17].

All mutants bound FAD to varying degrees with the exception of Glu39Gln and Glu39Ala (Fig. 2).

3.4. Serine 20

The residue Ser-20 was mutated to both an alanine and a threonine. Surprisingly, Ser20Ala bound FAD (0.7 × that of wild type), even with the removal of the polar side chain. However, a spectrophotometric scan from 550 to 300 nm showed a shift from the 375 to 360 nm peak in the case of Ser20Ala (Fig. 3). This alteration may be explained by the change in polarity of the residue or that the integrity of the bound FAD has been altered.

The UV/VIS spectrum of Ser20Thr was similar to that of wild type and this mutant was also able to bind FAD (to a similar degree as the Ser20Ala mutant). It is likely that, being a conservative change, the polar side chain of threonine is able to form polar

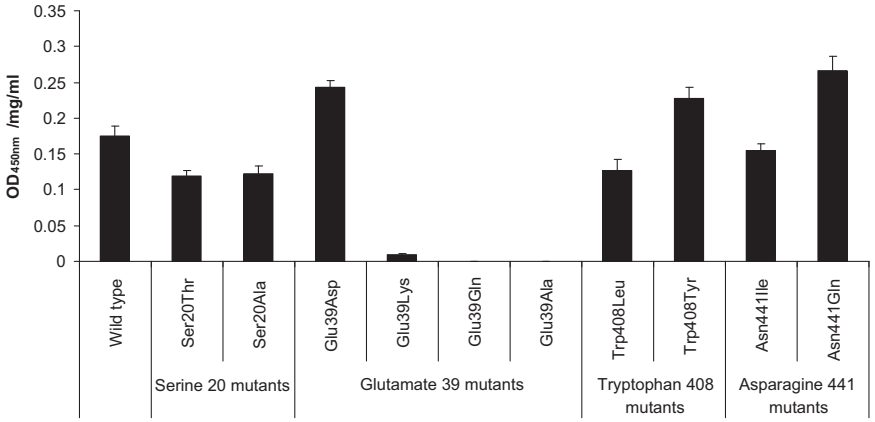

Fig. 2. FAD quantitation in MxPPOX protein; FAD absorbance at 450 nm was expressed as OD450 nm/mg of protein/ml. Data expressed as mean ± S.D., $n=3$.

Table 2
Kinetic parameters of wild type and mutant MxPPOX proteins. Results expressed as mean ± S.D. ($n=3$).

$n=3$	K_M (μM)	k_{cat} (s^{-1})	k_{cat}/K_M ($\mu M^{-1} s^{-1}$)	$T_{½}$
Wild type	0.38 ± 0.03	0.72 ± 0.06	1.88	50 ± 0.20
Ser20Thr	1.17 ± 0.04	0.78 ± 0.06	0.67	50 ± 0.50
Ser20Ala	0.92 ± 0.01	0.41 ± 0.02	0.45	56 ± 0.70
Glu39Asp	0.59 ± 0.03	1.52 ± 0.08	2.58	55 ± 0.10
Trp408Leu	0.51 ± 0.05	0.14 ± 0.01	0.28	52 ± 0.20
Trp408Tyr	1.49 ± 0.09	0.23 ± 0.04	0.15	56 ± 0.01
Asn441Ile	0.51 ± 0.02	0.08 ± 0.001	0.16	56 ± 0.50
Asn441Gln	0.75 ± 0.01	0.32 ± 0.01	0.43	50 ± 0.50

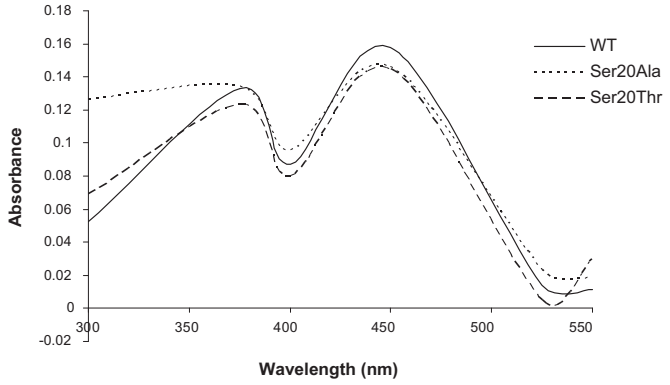

Fig. 3. UV/VIS spectra (300–550 nm) of wild type MxPPOX, Ser20Thr and Ser20Ala. Enzymes (~10 μM) were recorded in 50 mM $NaPO_4$ buffer pH 7.0, 0.5% Tween 20.

interactions with the FAD phosphate group as predicted in the wild-type (Fig. 1).

In order to investigate the spectral shift in Ser20Ala, a pH optimum analysis was performed on wild type MxPPOX and both serine mutants. This revealed both wild type and Ser20Thr to have a pH optimum of 8.1 whilst Ser20Ala, has a lower pH optimum at 7.5. This suggests that the polar group's interaction with FAD-phosphate may be important.

Furthermore, Ser20Ala has a $T_{½}$ of 56 °C confirming that this mutation has an influence on the structure–function relationship of the protein. The increase in $T_{½}$ could be attributable to the same properties resulting in the FAD spectral shift.

Ser20Thr had a similar catalytic turnover rate as wild type but a weaker substrate affinity (increased K_M); therefore, the overall catalytic efficiency was decreased compared to wild type (Table 2). Ser20Ala also had an increased K_M compared to wild type, affecting its catalytic efficiency but to a greater extent than in the case of the Ser20Thr. Compromised PPOX function in both mutants is also reflected in the lower specific activities, with Ser20Thr being slightly less affected than the Ser20Ala mutant. As a whole, these results suggest that a polar group may be more favourable at this position yet not essential.

3.5. Glutamate 39

Glutamate-39 is a polar negative residue that is hydrogen-bonded to the ribose ring of FAD; this conserved residue is the only residue interacting with the FAD ribose ring (Fig. 1). Such interaction (of a glutamate) is conserved in other PPOXs, as well as other oxidases in the same superfamily. The consensus sequence suggests that a glutamate or an aspartate is vital in this position. Indeed a recent publication by Shaub et al., [12] on the FAD-dependent oxidase, phytoene desaturase CRTI from Pantoeaananatis, noted that the superimposition of the individual domains of six Rossman fold proteins (including MxPPOX) showed nine residues making hydrophilic contacts with FAD. Of those nine only Glu39 (Glu31 in CRTI) makes side-chain only contacts with the ribose moiety, and is one of only six residues that are invariant in all six proteins.

In this study Glu-39 was mutated to an aspartate, lysine, glutamine and alanine. Glu39Asp bound FAD perfectly well, whereas Glu39Lys bound to a small extent (0.06 × that of wild type) (Figs. 2 and 4). PyMol simulation (data not shown), revealed this slightly bulky mutant to have inferior interaction with FAD. In the case of Glu39Gln and Glu39Ala no FAD bound. This implies that

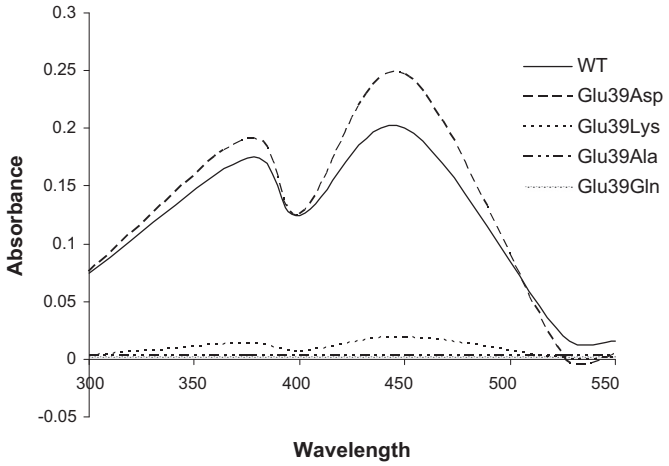

Fig. 4. UV/VIS spectra (300–550 nm) of wild type, Glu39Asp, Glu39Lys, Glu39Ala and Glu39Gln. Enzymes (~10 μM) were recorded in 50 mM $NaPO_4$ buffer pH 7.0, 0.5% Tween 20.

removal of the FAD–ribose ring interaction may compromise the remaining FAD interactions (such as interaction with the adenine ring, ribityl chain, isoalloxazine ring) to the extent that it is no longer able to bind and FAD dissociates readily. This phenomenon has previously been proposed [17,18].

Interestingly, kinetic analysis of Glu39Asp shows an increase in both k_{cat} and catalytic efficiency (k_{cat}/K_M) suggesting an almost fully functional enzyme. Thus a polar negatively charged residue clearly is favoured to interact with the FAD ribose ring.

Although the $T_{½}$ of Glu39Asp revealed an increased $T_{½}$, this change, which could be interpreted as indicating structural change in the active site, did not appear to have any major effect on substrate affinity. Removal of the negative charge, in mutants Glu39Gln, Glu39Ala, Glu39Lys resulted in a dramatic reduction in specific activity (hence kinetic parameters not determined) again suggesting the importance of the negative group's interaction with the ribose ring of FAD.

3.6. Asparagine 441

Asn-441 is positioned to interact via its side chain to possibly stabilise the ribityl chain of the FAD. A long loop located near the FAD twists perfectly to orientate the Asn-441 residue to interact with the phosphate group of the FAD via its side chain. Asn-441 also interacts with the ribityl chain of the FAD via its amino group. The Asn-441 residue was mutated to an isoleucine and a glutamine residue. Both Asn441Ile and Asn441Gln bound FAD at least as well as wild type, with similar UV/vis spectra, implying that a change in polarity in this region does not affect the ability to bind FAD (Fig. 5). Interestingly, Asn441Gln showed superior FAD binding to wild type.

PyMol simulation (data not shown) shows that Asn-441 makes two hydrogen bond interactions with the FAD ribityl group. PyMol simulation of the mutants revealed that the Asn441Gln mutant interacts with the phosphate rather than the ribityl chain. PyMol simulation of Asn441Ile showed that isoleucine was unable to make a hydrogen bond via its side chain with the ribityl chain of FAD. Since both mutants were able to bind FAD in the presence of an altered hydrogen bonding network, it is likely that Asn-441 is not involved in FAD binding directly but rather in stabilizing and orientating FAD.

Assessment of the kinetic behaviour revealed that both mutants were less efficient that wild type. The Asn441Ile showed an 11-fold decrease in catalytic efficiency compared to wild type as well as an increase in $T_{½}$. Asn441Gln, although less efficient than wild type protein, was more catalytically efficient than the

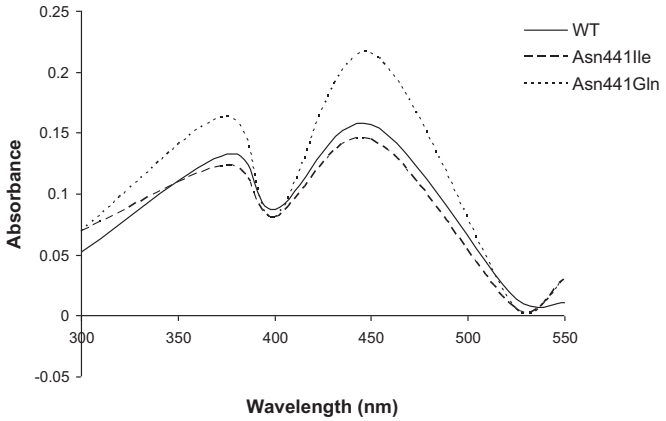

Fig. 5. UV/vis spectra (300–550 nm) of wild type, Asn441Gln and Asn441Ile (dotted lines). Enzymes (~10 μM) were recorded in 50 mM $NaPO_4$ buffer pH 7.0, 0.5% Tween 20.

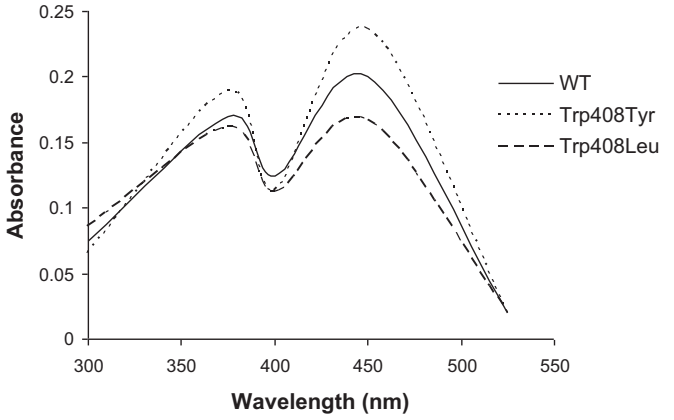

Fig. 6. UV/VIS spectra (300–530 nm) of wild type, Trp408Tyr and Trp408Leu. Enzymes (~10 μM) were recorded in 50 mM $NaPO_4$ buffer pH 7.0, 0.5% Tween 20.

Asn441Ile mutant. This highlights the importance of a polar side chain for efficiency and interaction with the ribityl chain of FAD. This conclusion is strengthened by our finding that Asn-441 is not involved in binding but rather in the alignment of FAD, as both mutants bound FAD.

3.7. Tryptophan 408

In MxPPOXs and related oxidases, a tryptophan residue is frequently seen near the isoalloxazine ring of FAD. A tryptophan residue, near the aromatic non-polar half of the isoalloxazine ring, has been hypothesised to interact via an aromatic–aromatic interaction to stabilise the bound FAD in other non-related flavoprotein oxidases [14,15]. In MxPPOX, although Trp-408 aligns with the tryptophan residues in BsPPOX and NtPPOX, the positioning of Trp-408 is further away from the isoalloxazine ring, suggesting, that in MxPPOX Trp-408 could have a different role. In this study Trp-408 was mutated to a leucine (non-polar linear) and a tyrosine (polar aromatic). Both mutants bound FAD (0.7 × and 1.3 × that of wild type for Trp408Leu and Trp408Tyr, respectively), and had a similar spectra to wild type MxPPOX (Figs. 2 and 6). Despite the removal of the aromatic ring, Trp408Leu showed a higher specific activity and a better substrate affinity (K_M) compared to Trp408Tyr although both were significantly less active and had a lower substrate affinity than wild-type. These effects are reflected in their respective catalytic turnover rates. This is also apparent in the $T_{½}$ values where Trp408Leu had a slightly increased $T_{½}$ and Trp408Tyr more so (Table 2).

These results suggest that a non-polar (or slightly polar) residue is favoured at this position with regards to activity and substrate affinity of the enzyme; however, the removal of the aromatic group resulted in a non-optimally functioning enzyme. In the strongly polar aromatic replacement (Trp408Tyr) both substrate affinity and enzyme efficiency was dramatically reduced compared to wild-type. Yet, spectral analysis of Trp408Tyr revealed that this polar aromatic is does not appear to affect the amount of bound FAD adversely (Figs. 2 and 6).

4. Conclusions

In this study we investigated the binding, orientation and stabilisation of FAD in MxPPOX by engineering mutants, modelling highly conserved residues that most likely interact with FAD via their side chains, and performing functional studies.

We have determined that the Ser-20 mutants studied do not affect FAD binding significantly and that polarity in this position

may be important for the integrity of FAD binding, yet not essential. By mutating Glu-39 we have also shown that a polar negatively charged residue clearly is favoured to interact with the FAD ribose ring. Asn-441 appears not to be involved in the binding of FAD directly, but in the orientation of the bound FAD and polarity in this position appears important for stabilizing the FAD. Our studies of the Trp408 mutants suggest that aromaticity in this position is not critical for functionality but that non- or slight-polarity is important.

This study suggests that the flavin mononuclotide (FMN) and adenosine diphosphate (ADP) moieties of FAD may play different roles in the FAD/protein interaction. The ADP which consists of adenine, ribose and a phosphate group may be involved in the binding of FAD to the protein. We propose that this region binds first to the protein followed by FMN′s interaction with the protein. FMN consists of the isoalloxazine ring, ribityl chain and a phosphate group. The ribityl group could be aligning the isoalloxazine ring of the FAD. Isoalloxazine is the reactive part of the FAD, receiving electrons from substrate, and hence its correct orientation and alignment is vital in mxPPOX for catalysis.

While this study focuses on characterising PPOX from *M. xanthus* it is possible that these findings may be extrapolated to the further understanding of the mechanism of PPOX catalysis, and in our understanding of PPOX mutant/disease function in variegate porphyria. It is entirely conceivable that mutations which affect the binding of FAD result in non-functional protein, leading to the build-up of porphyrin(ogen)s and potential VP symptomology.

Funding

This project was financed by the Medical Research Council, South Africa.

Acknowledgements

Thanks to Professor Harry Dailey and Tammy Dailey (Biomedical and Health Sciences Institute of Georgia, Athens, GA, USA) for providing us with the pMxPPOX vector.

Appendix A. Supplementary material

Supplementary data associated with this article can be found in the online version at http://dx.doi.org/10.1016/j.bbrep.2015.10.006.

References

[1] H.A. Dailey, Conversion of coproporphyrin to protoheme in higher eukaryotes: terminal three enzymes, in: H.A. Dailey (Ed.), Biosynthesis of Haem and Chlorophylls, McGraw-Hill, New York, 1990, pp. 123–161.
[2] M. Koch, C. Breithaupt, R. Kiefersauer, R. Huber, A. Messerschmidt, Crystal structure of protoporphyrinogen IX oxidase: a key enzyme in haem and chlorophyll biosynthesis, EMBO J. 23 (8) (2004) 1720–1728, http://dx.doi.org/10.1038/sj.emboj.7600189.
[3] H.R. Corradi, A.V. Corrigall, E. Boix, C.G. Mohan, E.D. Sturrock, P.N. Meissner, et al., Crystal structure of protoporphyrinogen oxidase from *Myxococcus xanthus* and its complex with the inhibitor acifluorfen, J. Biol. Chem. 281 (50) (2006) 38625–38633, http://dx.doi.org/10.1074/jbc.M606640200.
[4] X. Qin, L. Sun, X. Wen, X. Yang, Y. Tan, H. Jin, et al., Structural insight into unique properties of protoporphyrinogen oxidase from *Bacillus subtilis*, J. Struct. Biol. 170 (1) (2010) 76–82, http://dx.doi.org/10.1016/j.jsb.2009.11.012.
[5] X. Qin, Y. Tan, L. Wang, Z. Wang, B. Wang, X. Wen, et al., Structural insight into human variegate porphyria disease, FASEB J. 25 (2011) 653–664, http://dx.doi.org/10.1096/fj.10-170811.
[6] P.N. Meissner, A.V. Corrigall, R.J. Hift, Variegate porphyria, in: G.C. Ferreira (Ed.), Handbook of Porphyrin Science, vol. 29, World Scientific, 2013.
[7] R. Morgan, V. Silva, H. da, Puy, J. Deybach, G. Elder, Functional studies of mutations in the human protoporphyrinogen oxidase gene in variegate porphyria, Cell Mol. Biol. (noisy-le-grand) (2002) 4879–4882.
[8] I.U. Heinemann, N. Diekmann, A. Masoumi, M. Koch, A. Messerschmidt, M. Jahn, et al., Functional definition of the tobacco protoporphyrinogen IX oxidase substrate binding site, Biochem. J. (2007) 402575–402580, http://dx.doi.org/10.1042/BJ20061321.
[9] B. Wang, X. Wen, X. Qin, Z. Wang, Y. Tan, Y. Shen, Z. Xi, Quantitative structural insight into human variegate porphyria disease, J. Biol. Chem. 288 (2013) 11731–11740, http://dx.doi.org/10.1074/jbc.M113.45976.
[10] M.H. Maneli, A.V. Corrigall, H.H. Klump, L.M. Davids, R.E. Kirsch, P.N. Meissner, Kinetic and physical characterisation of recombinant wild-type and mutant human protoporphyrinogen oxidases, Biochim. Biophys. Acta (2003) 165010–165021, http://dx.doi.org/10.1016/S1570-9639(03)00186-9.
[11] T.A. Dailey, H.A. Dailey, Identification of an FAD superfamily containing protoporphyrinogen oxidases, monoamine oxidases and phytoene desaturase, J. Biol. Chem. 273 (22) (1998) 13658–13662, http://dx.doi.org/10.1074/jbc.273.22.13658.
[12] P. Schaub, Q. Yu, S. Gemmecker, P. Poussin-Courmontagne, J. Mailliot, A. G. McEwen, S. Ghisla, S. Al-Babili, J. Cavarelli, P. Beyer, On the structure and function of the phytoene desaturase CRTI from *Pantoea ananatis*, a membrane-peripheral and FAD-dependent oxidase/isomerase, PLoS One 7 (6) (2012) e39550, http://dx.doi.org/10.1371/journal.pone.0039550, Epub 2012 Jun 22.
[13] F. Dayan, P. Daga, S. Duke, R. Lee, P. Tranel, R. Doerksen, Biochemical and structural consequences of a glycine deletion in the alpha-8 helix of protoporphyrinogen oxidase, Biochim. Biophys. Acta 180 (4) (2010) 1548–1556, http://dx.doi.org/10.1016/j.bbapap.2010.04.004.
[14] C. Binda, A. Coda, R. Angelini, R. Federico, P. Ascenzi, A. Mattevi, A 30 A long U-shaped catalytic tunnel in the crystal structure of polyamine oxidase, Structure 7 (3) (1999) 265–275.
[15] R. Neeli, O. Roitel, N.S. Scrutton, A.W. Munro, Switching pyridine nucleotide specificity in P450 BM3, J. Biol. Chem. 280 (18) (2005) 17634–17644, http://dx.doi.org/10.1074/jbc.M413826200.
[16] J. Kane, D. Hartley, Properties of inclusion bodies from recombinant *Escherichia coli*, Biochem. Soc. Trans. 16 (2) (1988) 101–102.
[17] T.A. Dailey, H.A. Dailey, Human protoporphyrinogen oxidase: expression, purification, and characterization of the cloned enzyme, Protein Sci. 5 (1996) 98–105, http://dx.doi.org/10.1002/pro.5560050112.
[18] H.A. Dailey, T.A. Dailey, Protoporphyrinogen oxidase of *Myxococcus xanthus*: expression, purification and characterisation of the cloned enzyme, Biochemistry 271 (15) (1996) 8714–8718, http://dx.doi.org/10.1074/jbc.271.15.8714.